

Net Terrestrial Radiative Heat Fluxes over India during Monsoon

R. V. GODBOLE and R. R. KELKAR

Institute of Tropical Meteorology, Poona

(Received 15 April 1968)

ABSTRACT. Infra-red radiative heat flux and instantaneous rate of temperature change have been computed for Indian sub-continent for monsoon season by making use of the numerical method developed for the purpose. The effects of water vapour alone have been considered. It is found that the radiative heat loss near the surface is minimum over the Western Ghats. Over northeast and northwest India, the radiative heat loss is relatively high. Also, the radiative cooling integrated from the surface upto 300 mb indicates a large cooling over northeast and northwest India ($>1^{\circ}\text{C}$ per day) and relatively small cooling over the southern Peninsula ($<0.25^{\circ}\text{C}$ per day). Analysis of the day-to-day values of net flux and temperature suggest no cause-and-effect relationship. However, a good correspondence has been noticed between net flux, temperature and total moisture content as far as surface level is concerned. The day-to-day values of net flux at higher levels follow very closely to those at the surface.

1. Introduction

Until recently, studies on the distribution of terrestrial radiative heat flux near the earth's surface and at various levels in the atmosphere had received very little attention. The meteorological satellites afforded, for the first time, means to study the distribution of radiative heat losses on a global scale. The pyrgeometers, which have been recently set up as part of the global radiation network programme, provide another means to study the configuration of radiative heat flux with respect to space and time. Using Angstrom Pyrgeometers, Mani, Chacko and Iyer (1965) have presented the distribution of terrestrial radiation over the Indian region. The pyrgeometer, however, can only be used on clear nights when the wind is light. Also it estimates the net upward radiative heat loss only from the earth's surface. The satellite, on the other hand, estimates the radiative heat loss from the earth-atmosphere system as a whole, to outer space. These techniques, therefore, provide no knowledge about the radiative exchange processes operating at the intermediate levels. The radio-meter-sondes would overcome this difficulty but unfortunately, they have not been introduced on a routine operational basis, with a network of observations sufficient to facilitate the study of the distribution pattern of radiative heat flux.

M/P(N)76DGOB

It is possible to calculate the radiative heat fluxes at various levels in the atmosphere by indirect methods, such as the graphical methods developed by Elsasser (1942) and Yamamoto (1952). Using Elsasser's graphical method, Godbole (1963) had studied the distribution of radiative heat flux with respect to mobile cyclone systems in the North Atlantic. The graphical methods, however, are time consuming and it is almost impossible to use these to make a systematic study over large regions or over long periods of time.

In the present work, a numerical method has been developed and used in place of the graphical method. Computations have been carried out partly on IBM 1620 at the Institute of Tropical Meteorology, Poona and partly on CDC 3600 at the Tata Institute of Fundamental Research, Bombay. The *Atmospheric radiation tables* by Elsasser and Culbertson (1960) have been used for numerical integration. Infra-red radiative heat fluxes in the upward and downward directions have been computed at the earth's surface and at standard isobaric levels for thirteen Indian radiosonde stations for a typical monsoon month, namely, July 1962. The computations have been carried out on a day-to-day basis so that the influence of radiative processes on day-to-day temperature fluctuations could be examined.

Mean values of the net flux at the earth's surface and at 850, 700, 500 and 300 mb have been analysed. Only the effects due to the absorption of water vapour have been considered, since our interest has been confined, for the time being, upto 200 mb in the vertical.

The presence of clouds has been taken into account. For a cloud cover less than 100 per cent, a prorated amount of flux is computed from the flux for overcast and cloudless sky conditions. The height of the base of the cloud needed in the computation has been taken as reported. However, the top of the cloud has been considered at either 400 or 200 mb depending upon whether cloud reported is medium or high.

2. Flux of Terrestrial Radiation

By solving the equation of radiative heat transfer with the boundary condition that downward long-wave radiation is zero at the top of the atmosphere, the downward flux of radiation at height Z , due to any absorption band may be expressed as —

$$D_Z = \int_{T_Z}^{T_0} \left[\int_{\nu_1}^{\nu_2} \frac{dB_\nu}{dT} \left\{ 1 - \tau_f(k_\nu, u) \right\} d\nu \right] dT + \int_{T_0}^0 \left[\int_{\nu_1}^{\nu_2} \frac{dB_\nu}{dT} \left\{ 1 - \tau_f(k_\nu, u) \right\} d\nu \right] dT \quad (1)$$

Also, assuming that the upward radiation at the earth's surface is equal to the black body radiation at surface temperature, the upward flux of radiation at any height Z may be similarly obtained as —

$$U_Z = \sigma T_G^4 - \int_{T_Z}^{T_G} \left[\int_{\nu_1}^{\nu_2} \frac{dB_\nu}{dT} \left\{ 1 - \tau_f(k_\nu, u) \right\} d\nu \right] dT \quad (2)$$

Here, T_0 is the temperature at the top of the atmosphere, T_Z the temperature at any reference height Z and T_G the temperature of the earth's surface. B_ν is the monochromatic black body flux, σ the Stefan-Boltzman constant, and ν_1 and ν_2 are the band limits expressed in wave number. τ_f is the generalized transmission function representing a fractional transmission of monochromatic radiation through optical depth u , and k_ν is the absorption coefficient of water vapour at wave number ν .

Following Elsasser and Culbertson (1960), the above equation can be written as —

$$D_Z = \int_{T_Z}^{T_0} R[u(T), T] dT + \int_{T_0}^0 R[u_0(T_0), T] dT \quad (3)$$

$$U_Z = \sigma T_G^4 - \int_{T_Z}^{T_G} R[u(T), T] dT \quad (4)$$

where,

$$R(u, T) = \int_{\nu_1}^{\nu_2} \frac{dB_\nu}{dT} \left\{ 1 - \tau_f(k_\nu, u) \right\} d\nu \quad (5)$$

The net radiative heat flux at any height Z is

$$N_Z = U_Z - D_Z \quad (6)$$

The net flux is, under normal circumstances, in the upward direction at any height.

Values of $R[u, T]$ defined above, have been tabulated by Elsasser and Culbertson as functions of temperature and effective optical depth. In the present computational scheme, the optical depth for each level with respect to the reference level has been obtained. $R[u, T]$ is then interpolated for the corresponding optical depth and temperature. The numerical integration of $R[u, T]$ with respect to T , i.e., $\int R dT$ would eventually give either downward or upward flux.

The optical depth for any absorbing gas in a layer of thickness ΔZ is given by —

$$\Delta u = \rho_G \Delta Z \quad (7)$$

where ρ_G is the density of the absorbing gas. For water vapour considerations alone, ρ_G is replaced by ρr , ρ being the density of air and r is the water vapour mixing ratio. Using the hydrostatic relation, equation (7) may be rewritten as —

$$\Delta u = \frac{1}{g} r \Delta p \quad (8)$$

The optical depth is further multiplied by a pressure correcting factor (p/p_0) to obtain the effective optical depth given by —

$$\Delta u = \frac{1}{g} r \Delta p (p/p_0) \quad (9)$$

For computation of optical depth, the upper limit of the atmosphere has been considered at 200 mb. Above 500 mb, the optical depth is obtained by extrapolation (see Appendix).

3. Radiative cooling

If N_1 and N_2 are the net fluxes of radiative heat at levels 1 and 2 respectively of a horizontally

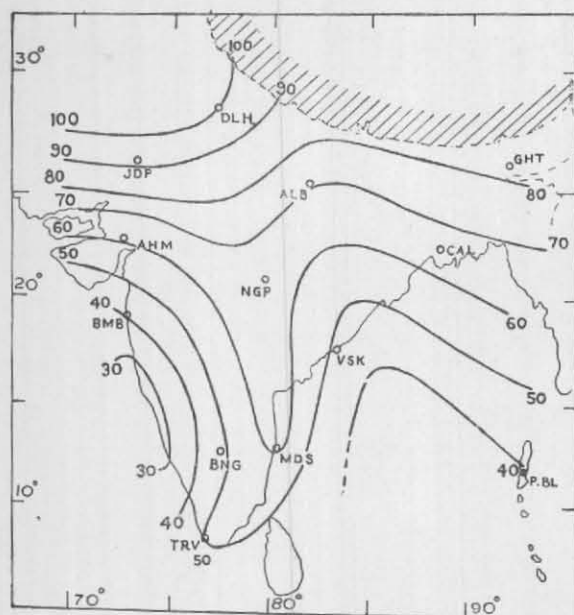


Fig. 1(a). Distribution of net radiative heat flux (with clouds) at the surface (Mean for July 1962)
Unit : 10^{-3} ly per min

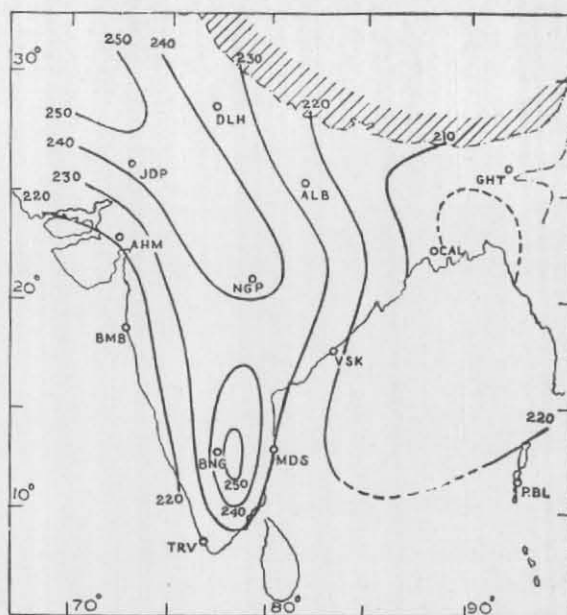


Fig. 1(b). Distribution of net radiative heat flux (without clouds) at the surface (Mean for July 1962)
Unit : 10^{-3} ly per min

uniform layer of thickness ΔZ , the net heating rate is given by —

$$\frac{\Delta Q}{\Delta t} = (N_1 - N_2) / \Delta Z \quad (10)$$

where ΔQ is the amount of heat accumulated in a unit volume in time Δt . From the first law of thermodynamics, neglecting pressure expansion, we get —

$$\begin{aligned} \frac{\Delta Q}{\Delta t} &= \rho C_p \frac{\Delta T}{\Delta t} = \frac{N_1 - N_2}{\Delta Z} \\ \frac{\Delta T}{\Delta t} &= \frac{g}{C_p} \frac{N_1 - N_2}{p_1 - p_2} \end{aligned} \quad (11)$$

Here, p_1 and p_2 are pressures at levels 1 and 2 respectively. For the convergence of the flux, $N_1 > N_2$, $\Delta Q / \Delta t > 0$ and there is a radiative warming. For $N_1 < N_2$ there is a radiative cooling of the atmosphere.

4. Results and Discussion

Radiative heat flux — Fig. 1(a) shows the distribution of net radiative heat flux at the surface taking into account the presence of clouds. It is seen that the Western Ghats lose relatively small amount of radiation (0.03 ly per min). High value (0.1 ly per min) are found in the north-west corner, with a ridge extending down to the south. In the south central region, the gradient is rather flat. On the whole, the pattern seems to reflect the effect of continentality and topography.

The distribution of net radiative heat flux disregarding cloud is shown in Fig. 1(b). Here, the flux values are uniformly high all over as compared to those with cloud cover (Fig. 1a). This is obvious because a cloud layer, acting like a black body, keeps the atmosphere below it relatively warm. The ridge of high values in Fig. 1(b) extends further south, merging into a secondary maximum (0.25 ly per min) located close to Bangalore. The south central region is again characterised by a flat gradient. The low values (0.2 ly per min) on the east as seen in Fig. 1(b) are absent in Fig. 1(a). In order to understand these features, it would be expedient to examine the distribution of such parameters as surface temperature, water vapour and cloud amount (Fig. 2).

Northwest India is characterised by high surface temperature, low moisture content, and small cloud amount as a result of which the radiation loss at the surface is relatively high. Also, over the west coast, the surface temperature is usually at a minimum, the air is laden with moisture and the total cloud amount is large; these conditions account for the low values of flux shown in Figs. 1(a) and 1(b). The large radiation loss in the vicinity of Bangalore (Fig. 1b) is seen to be due to low moisture (Fig. 2c) and high surface temperature (Fig. 2a). The centre of low flux values over Assam in Fig. 1(b), is mainly due to the large moisture content (Fig. 2c). Although it is apparent that the presence of cloud considerably decreases the flux

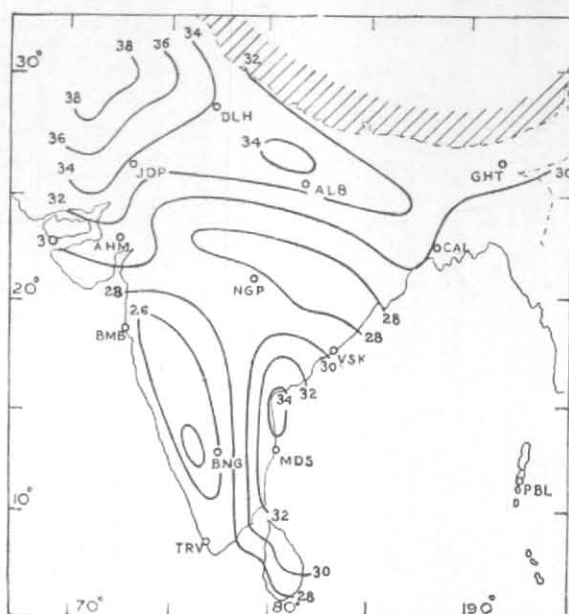


Fig. 2(a). Distribution of temperature ($^{\circ}\text{C}$) at the surface
(Mean for July 1962)

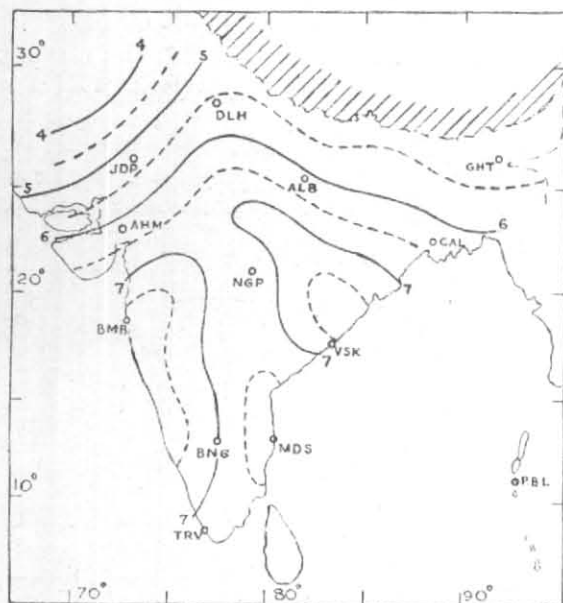


Fig. 2(b). Distribution of cloud amount (in eighths)
(Mean for July 1962)

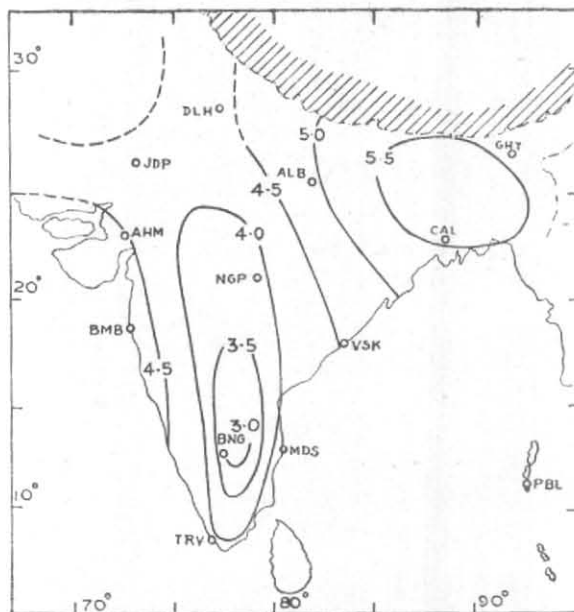


Fig. 2(c). Distribution of optical depths (gm cm^{-2}) measured
from the ground
(Mean for July 1962)

values all over the Indian region, its modifying influence is clearly discernible in the vicinity of Visakhapatnam (Fig. 2b). Here, a patch of large amount of cloud protrudes inland which tends to create a similar protrusion in the radiative flux pattern of Fig. 1(a).

The mean net radiative heat flux at 850, 700, 500 and 300 mb is shown in Figs. 3(a), 3(b), 3(c) and 3(d) respectively. It is seen that the principal regions characterising high and low values of net flux at the surface remain more or less at higher levels also.

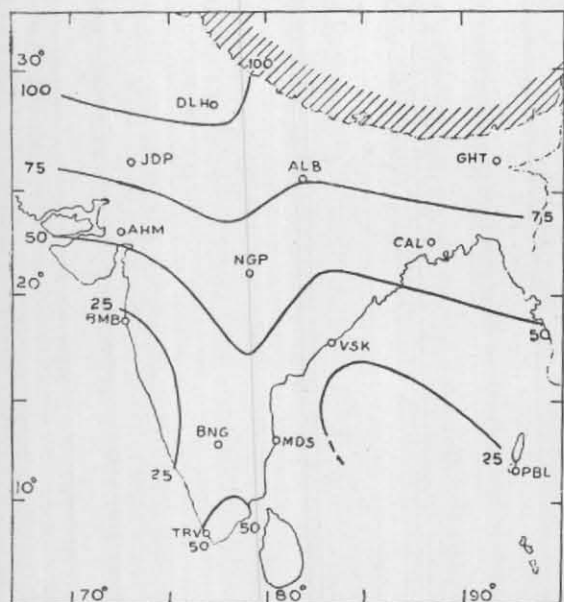


Fig. 3(a). 850 mb

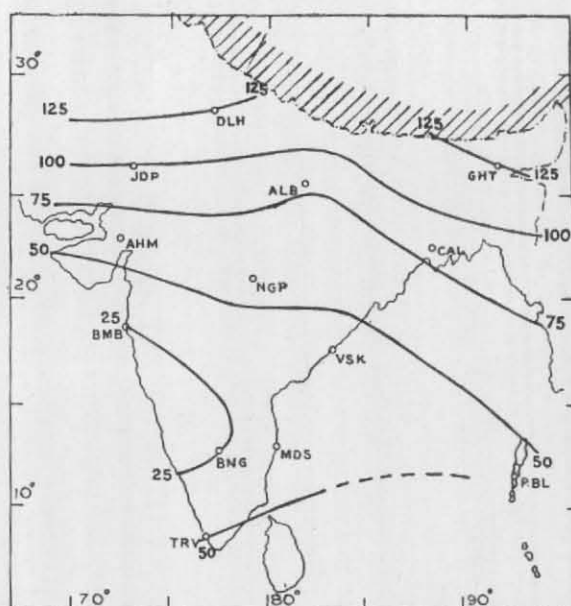


Fig. 3(b). 700 mb

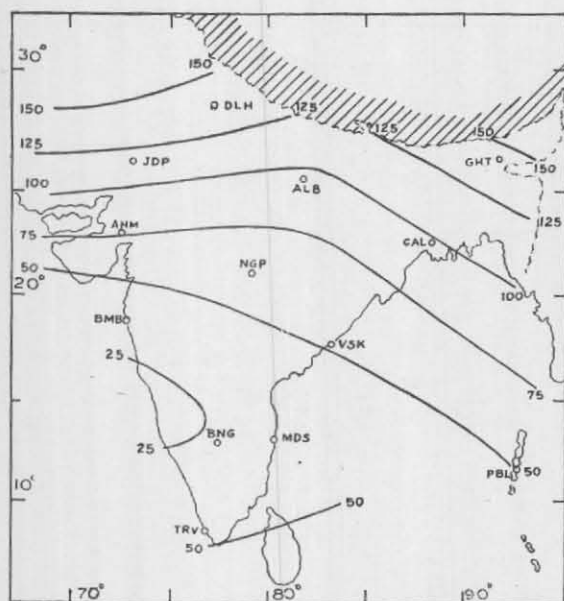


Fig. 3(c). 500 mb

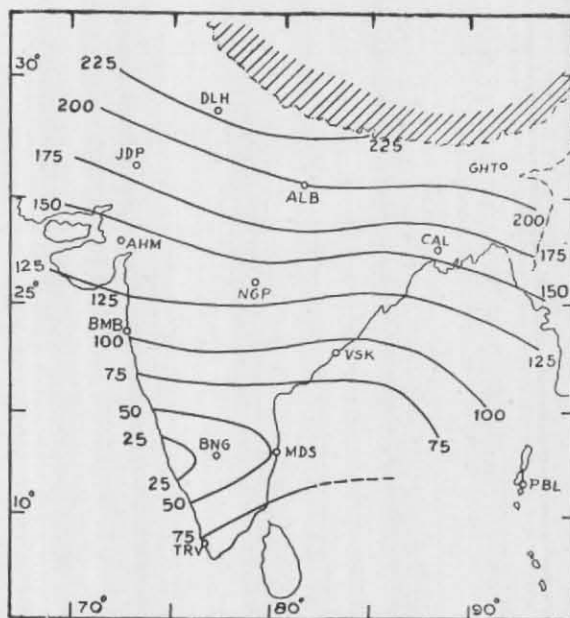


Fig. 3(d). 300 mb

Fig. 3. Distribution of net radiative heat flux (with clouds) at 850, 700, 500 and 300 mb (Mean for July 1962)

Unit : 10^{-3} ly per min

The magnitudes of the flux at 850 mb are slightly smaller than at the surface especially over the Peninsula. This decrease in the magnitude could be accounted for mainly by the large amount of cloud and low cloud base which is normally observed over the southern Peninsula during early monsoon.

The distribution pattern begins to change from 700 mb upward (Figs. 3b, 3c, 3d). The ocean-continent influences appear to become less noticeable while the meridional gradient gains in strength. This is clearly seen at the 300-mb level (Fig. 3d), where the flux isopleths are more closely packed and tend to be parallel to the latitudes.

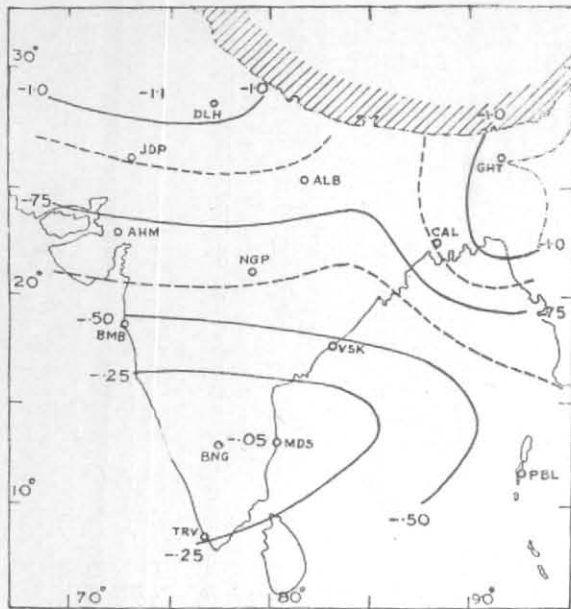


Fig. 4. Distribution of radiative cooling in a layer from the surface to 300 mb
Unit: °C per day

It is interesting to note from Figs. 3(a) to 3(d) that the net flux increases with height everywhere except over a small portion of the west coast where the lowest value (0.025 ly per min) persists at all levels from the surface upto 300 mb. This feature may be explained as follows. In a cloudless atmosphere, under normal conditions (in which the moisture decreases with height), the net flux increases with height. In the presence of clouds, however, the net flux at any height inside the cloud layer is obviously zero. Over the western coast, in addition to the cloud amount being large, the cloud layer is observed to be very deep invariably extending beyond 300 mb. This accounts for the low values of the net flux over the west coast at almost all the levels.

Radiative Cooling — The integrated cooling from the surface to 300 mb has been calculated and shown in Fig. 4. In this connection the values of the net flux (Figs. 1a and 3a to 3d) at grid points of five-degree latitude-longitude interval, have been considered. Also, a proper weight factor for each layer has been given.

It is seen that cooling of as much as 1.1 to 1.2°C per day takes place over the region of northeast and northwest India. On the other hand, the southern Peninsula exhibits a much smaller degree of cooling which is 0.25°C or less per day. Since the cooling pattern is actually derived from the distribution of the net radiation at various isobaric

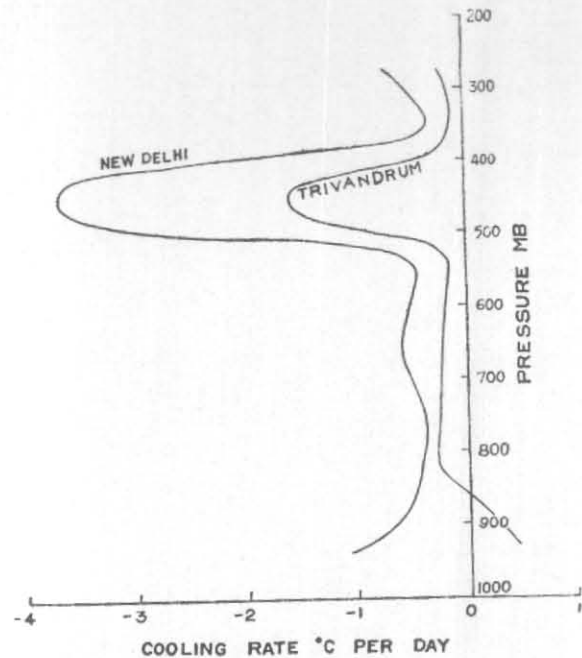


Fig. 5. Rate of temperature rate (°C per day) along the vertical for New Delhi and Trivandrum

levels it reflects what has already been discussed in the foregoing section. High moisture content and large amount of deep cloud layers in the south tend to minimize the heat loss to outer space, whereas high temperature and small cloud amount seem to be mainly responsible for a large cooling in the north.

The variation of rate of cooling with height is shown in Fig. 5 for two stations, New Delhi and Trivandrum. The effect of cloud has been taken into account. It may be noted that the temperature changes shown are the mean of day-to-day temperature changes (with cloud) for the month of July.

It is seen that at Trivandrum, there is a little warming (0.5°C per day) which decreases with height in the lower layers above the surface. In other words, there is a relative cooling with height in the lower layers. This is clearly due to the presence of clouds having very low base. On the other hand, at New Delhi, the cooling rate decreases with height, from 1.2°C per day to about 0.5°C per day in the lower layers. This is because, at New Delhi, large amounts of clouds do not occur frequently, and the clouds that form have a rather high base (above 800 mb).

For a layer from 800 to 550 mb, the cooling rate is very small at both the stations; that at New

Delhi being slightly large. The fact that cooling rate at any level within the cloud layer is zero, would give rise to such small cooling. The conspicuous feature of Fig. 5 is the large cooling both at New Delhi and Trivandrum at about 450 mb. The cooling rate at New Delhi is considerably higher (3.7°C per day) than that at Trivandrum (1.7°C per day) which only means that the cloud top at New Delhi loses black body heat at higher temperature than that at Trivandrum. Beyond 350 mb the cooling rate increases because of a rapid decrease of water vapour mixing ratio with height.

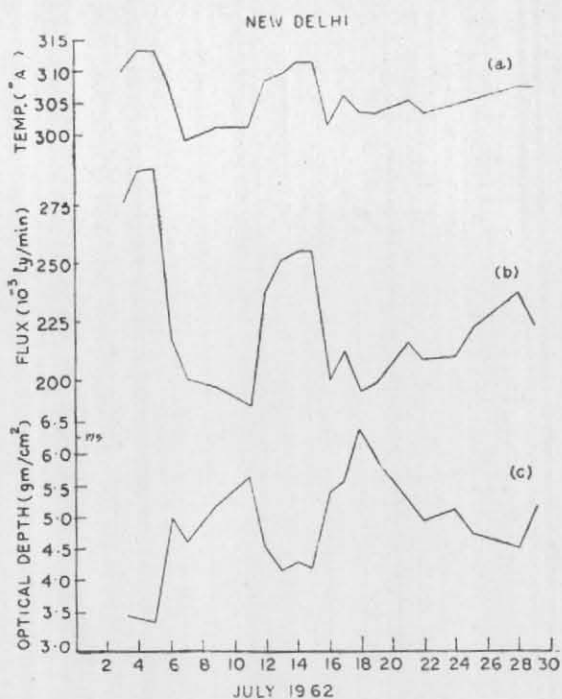
Day-to-day variations — It would be interesting to see how the general features discussed above hold good if considered on a day-to-day basis for individual stations. With this objective in view, day-to-day radiative heat fluxes at the surface have been critically examined for two representative stations, *viz.*, New Delhi and Calcutta. Also, the day-to-day flux values for higher levels as obtained for New Delhi have been considered.

It is seen from Fig. 6 that the net flux varies directly with temperature and inversely with optical depth. The net flux varies over a range of 190 to 290 ly per min at New Delhi in contrast with the flux range of 190 to 225 ly per min noticed at Calcutta. At New Delhi (Fig. 6a) the variations in temperature and optical depth have large amplitude as compared to those at Calcutta (Fig. 6b). Further it is of interest to note that the optical depth at Calcutta undergoes more rapid fluctuations than those at New Delhi, and this feature has been rightly reflected in the variation of the net flux at these stations.

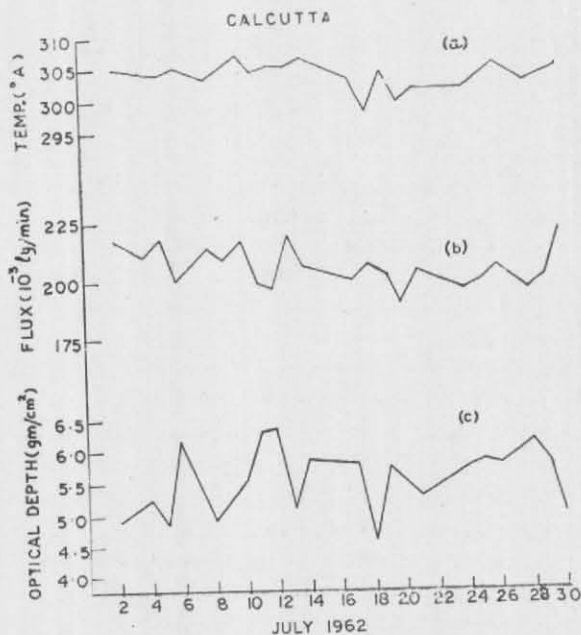
The day-to-day variation of the net flux at various levels in the atmosphere from ground upto 300 mb for New Delhi is shown in Fig. 7. The striking feature of the diagram is the close correspondence of the variation of the net flux at higher levels in tune with that at the surface. This immediately suggests, on the basis of Fig. 6, that optical depth and temperature variations at higher levels should follow a similar pattern. A cursory examination of optical depths and temperatures for various reference levels in the free atmosphere for New Delhi for the period under question indicated that the inference was valid for optical depth but not for temperature. The analysis has not been presented in the paper because this aspect of study which has important implications calls for a more careful examination on a rather comprehensive scale.

5. Conclusions

It has been shown that the distribution of the flux at surface and at higher levels in the atmosphere is a consequence of the distribution of



(a) At New Delhi



(b) At Calcutta

Fig. 6 Day-to-day values of (a) surface temperature, (b) surface net flux and (c) optical depth above the surface

temperature, water vapour and clouds. Near the coast where the moisture content of the atmosphere is high, the loss of radiative heat is small as compared to that over the inland region (north-west India) where the temperature is high and moisture content and cloudiness is low.

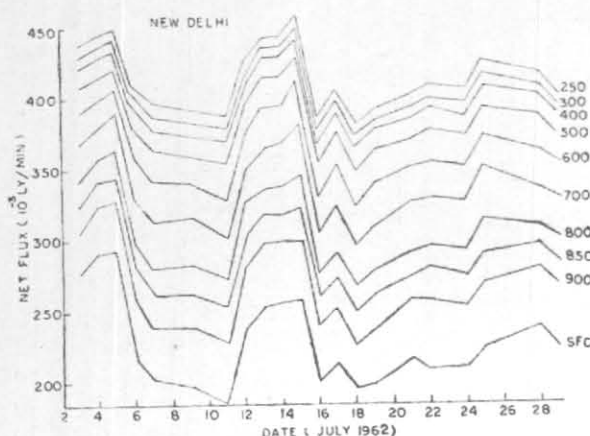


Fig. 7. Day-to-day values of net flux (without clouds) at various levels from surface to 200 mb at New Delhi

The day-to-day variation of the net flux at the surface follows closely that of the surface temperature and inversely that of optical depth above the surface. Also, the variation of the net flux at higher levels closely follows the surface net flux.

In the present investigation, the heat transfer has been considered to be due to water vapour alone, because in the troposphere, the contribution due to water vapour is, by far, the largest. It is intended to incorporate the effects due to carbon dioxide and ozone in future studies.

In the computations, the height of the base of low clouds has been taken as reported in the *Indian Daily Weather Report* published by the India Meteorological Department. These heights are based only on visual estimates and hence to that extent the correctness in the present computations is affected. Similar uncertainty exists in the consideration of the height of the cloud top.

While examining the cooling curve for New Delhi and Trivandrum in Fig. 5, it was found from the daily radiosonde data that the difference in temperatures at 400 mb for New Delhi and Trivandrum is sometimes as large as 10°C . While such a large temperature difference may perhaps

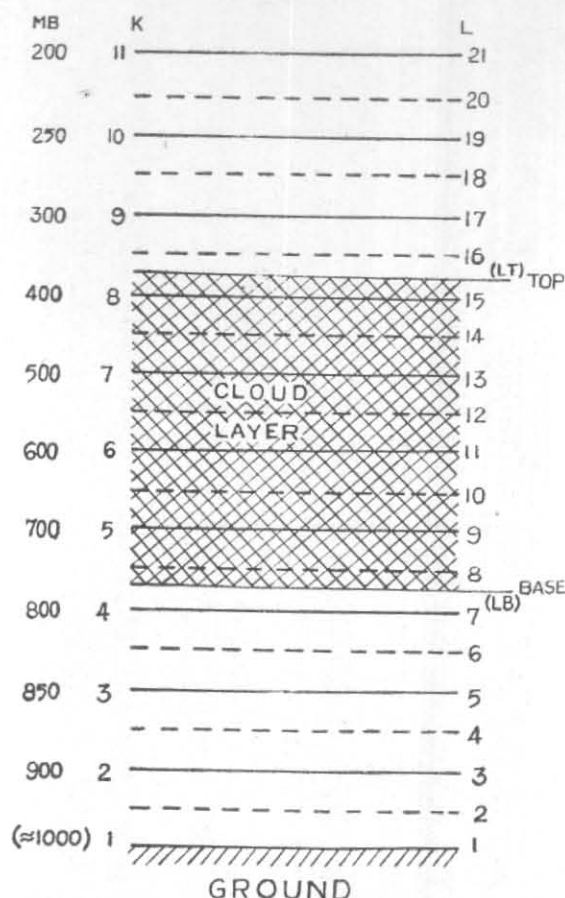


Fig. 8. The atmosphere divided into 20 layers from the surface to 200 mb

K—levels denote reference levels at which fluxes are computed

be real, it may be noted that instruments used for aerological soundings at the two places are of different types.

6. Acknowledgement

The authors wish to express their sincere thanks to Dr. Bh. V. Ramana Murty for his interest in the study, for going through the manuscript, and for making useful suggestions. Thanks are also due to Shri K. V. S. Madhavan and Miss S. M. Bakre for typing the manuscript and to our colleagues in the Drawing Section for preparing the diagrams.

REFERENCES

- | | | |
|---------------------------------------|------|--|
| Elsasser, W. M. | 1942 | <i>Heat transfer by infra-red radiation in the atmosphere</i> , Harvard Met. Studies, 6, p. 107. |
| Elsasser, W. M. and Culbertson, M. F. | 1960 | <i>Atmospheric radiation tables</i> , Met. Monographs No. 23, Boston, Amer. met. Soc., p. 43. |
| Godbole, R. V. | 1963 | <i>J. appl. Met.</i> , 2, p. 674. |
| Mani, A., Chacko, O. and Iyer, N. V. | 1965 | <i>Indian J. Met. Geophys.</i> , 16, p. 445. |
| Yamamoto, G. | 1952 | <i>On a radiation chart</i> , Sci. Rep. Tohoku Univ., Ser. 5, Geophys., 4, p. 9. |

APPENDIX

Computation Scheme

We define

$$R'(u, T) = \int_0^T R(u, T) dT = \int_0^{193} R(u, T) dT + \int_{193}^T R(u, T) dT \quad (1)$$

$$= R'(u, 193^\circ \text{K}) + \sum_{T=203,10}^{313} \frac{R(u, T) + R(u, T-10)}{2} \Delta T \quad (2)$$

where $\Delta T = 10^\circ \text{K}$. Values of $R'(u, 193^\circ \text{K})$ and $R(u, T)$ for $T = 193^\circ \text{K}$ to 313°K have been tabulated by Elsasser and Culbertson.

We divide the atmosphere from the ground upto 200 mb into 20 layers as shown in Fig. 8 and define —

$$L = 2k - 1, \quad k = 1, 11 \quad (3)$$

where k is the reference level ($k = 1$ for the ground). Values of u_{kL} corresponding reference level k and T_L are defined for $L = 1, 21$.

Clear sky—In the following the superscript c stands for clear sky condition. The downward flux at any reference level k is given by —

$$D_k^c = \sum_{L=2k-1}^{20} \left\{ R' \left(\frac{u_{kL} + u_{k,L+1}}{2}, T_L \right) - R' \left(\frac{u_{k,L} + u_{k,L+1}}{2}, T_{L+1} \right) \right\} + R'(u_{k,21}, T_{21}), \quad (4)$$

$k = 1, 10$

The upward flux at the ground is given by —

$$U_1^c = \sigma T_1^4 \quad (5)$$

and at any reference level k —

$$U_k^c = \sigma T_1^4 - \sum_{L=1}^{2k-2} \left\{ R' \left(\frac{u_{k,L} + u_{k,L+1}}{2}, T_L \right) - R' \left(\frac{u_{k,L} + u_{k,L+1}}{2}, T_{L+1} \right) \right\}, \quad k = 2, 11 \quad (6)$$

The net flux is given by —

$$N_k^c = U_k^c - D_k^c \quad (7)$$

Overcast sky—In the following the superscript o stands for overcast sky condition. The downward flux at any reference level k is given by —

$$D_k^o = D_k^c, \quad \text{if } k \text{ is above the cloud top} \quad (8)$$

$$D_k^o = \sigma T_{2k-1}^4, \quad \text{if } k \text{ is within the cloud layer} \quad (9)$$

For k below the cloud base —

$$D_k^o = \sum_{L=2k-1}^{LB-1} \left\{ R' \left(\frac{u_{k,L} + u_{k,L+1}}{2}, T_L \right) - R' \left(\frac{u_{k,L} + u_{k,L+1}}{2}, T_{L+1} \right) \right\} + \left\{ R' \left(\frac{u_{k,LB} + u_{k,BASE}}{2}, T_{LB} \right) - R' \left(\frac{u_{k,LB} + u_{k,BASE}}{2}, T_{BASE} \right) \right\} + \sigma T_{BASE}^4 \quad (10)$$

where, LB is the L -level immediately below the cloud base.

The upward flux is given by —

$$U_k^o = U_k^c, \quad \text{if } k \text{ is below the cloud base} \quad (11)$$

$$U_k^o = \sigma T_{2k-1}^4, \quad \text{if } k \text{ is within the cloud layer} \quad (12)$$

For k above the cloud top

$$U_k^o = \sigma T_{\text{TOP}}^4 - \left\{ R' \left(\frac{u_{k,LT} + u_{k,\text{TOP}}}{2}, T_{LT} \right) - R' \left(\frac{u_{k,LT} + u_{k,\text{TOP}}}{2}, T_{\text{TOP}} \right) \right\} - \sum_{L=LT}^{2k-2} \left\{ R' \left(\frac{u_{k,L} + u_{k,L+1}}{2}, T_L \right) - R' \left(\frac{u_{k,L} + u_{k,L+1}}{2}, T_{L+1} \right) \right\} \quad (13)$$

Here, LT is the L -level immediately above the cloud top.

The net flux is given by—

$$N_k^o = U_k^o - D_k^o \quad (14)$$

Prorated flux — If n is the amount of cloud reported, the prorated net flux is —

$$N_k^P = \frac{n N_k^o + (8-n) N_k^c}{8} \quad (15)$$

Similar expressions hold good for the prorated downward and upward flux.